Investigation of a Large-Mode-Area Fiber Designed for 2.0 μm Based on Multi-Layer Holes Resonance

Xiao Shen, Yifei Sun, Meimei Kong, and Wei Wei

***Abstract*—This work proposes a novel large mode area fiber with multi-layer holes of 2.0 μm based on electromagnetic field theory and finite element analysis. Modifying the structure parameters can reduce the fundamental mode confinement loss to less than 0.1 dB/m, and the lowest high-order mode confinement loss may be greater than 10.0 dB/m. The fiber has exceptional single-mode transmission performance due to its high loss ratio. The effective mode field area is 3849 μm^2, and the single mode core diameter is 80.0 μm. To obtain a larger mode field diameter, the construction used here includes a smaller cladding diameter in the already available large mode field fiber. The cladding parameters may be changed independently, making it convenient and adaptable to obtain the best simulation results. Compared to the large-mode field fiber standard, which has excellent single mode operation performance, the loss ratio of this design is substantially larger. Additionally, it can effectively sustain single mode operation when the wavelength shifts from 1.65 to 2.10 μm, which is advantageous for developing 2.0 μm fiber lasers.**

***Index Terms*—Fiber laser, large mode area fiber, transmission characteristics.**

TABLE I
PERFORMANCE COMPARISON OF FIBER MODELS

Fiber models	Transmission characteristics			
	L_{01} (dB/m)	L_{11} (dB/m)	A_{eff} (μm^2)	bend radius (cm)
LC-PBGF[12]	0.012	5.94	900	45
MTF[13]	0.07	39	630	20
PCF[14]	0.064	20	974	15
HIRR-SCF[15]	0.095	2.62	835	15
HHCF[16]	0.093	9.47	2025	-
LPF[17]	0.06	9	33000	-
PBF[18-19]	0.023	23	531	-
LCF[20]	0.1	1	1440	-

I. INTRODUCTION

MEDICAL surgery, industrial processing, atmospheric sensing, optical communication, and detection depend on 2.0 μm Tm^{3+}-doped fiber lasers [1], [2], [3], [4], [5], [6], [7]. After thirty years of rapid growth, Tm^{3+}-doped fiber lasers have attained kilowatt-level power [8], [9], [10]. However, the fiber laser suffers from severe quantum loss and prominent nonlinear effects caused by thermal effects due to the large wavelength gap between the pump wavelength (793 nm) and the signal light wavelength (2000 nm), which restricts further increases of the laser power level. Increasing the size of the mode field is the most efficient technique to address this issue of high power density. Nevertheless, it introduces negative impacts including poor beam quality and an increase in high-order modes (HOMs) [11].

Numerous novel large mode field area (MFA) and single mode fibers have been created. They have been used differently to increase MFA and achieve single mode characteristics, and their performances are listed in Table I. Some of these designs achieve single-mode characteristics by bending characteristics to increase losses. For example, X Chen et al. created a novel all-solid-state single-mode large-mode-field fiber in 2021 [12], the MFA was 900 μm^2, and the bending radius was 45 cm. In 2014, Deepak Jain et al. created a multitrench fiber that achieved an MFA of 630 μm^2 at a bending radius of 20 cm [13]. The MFA is not large enough to decrease the laser power density. That same year, a triangular-core photonic crystal fiber was also designed by the team of Saini T S [14]. The achieved MFA is 974 μm^2 at a bending radius of 15 cm. In 2021, Li Pei's team designed a segmented cladding fiber with high-index rings in the core (HIRRR-SCF) [15]. The MFA is 835 μm^2 at a bending radius of 15 cm; however, its loss ratio (LR) is also small due to its large fundamental mode (FM) loss and small HOM loss.

The above optical fibers all rely on the bending effect to achieve high-order mode filtering, but some fibers do not require bending to achieve the same goal. In 2021, our team proposed a heterogeneous helical cladding (HHC) fiber [16]. The MFA is 2025 μm^2, and the loss of HOMs is relatively low, which needs a longer fiber to filter out HOMs. In 2019, Fabian Stutzki's team proposed the Large Pitch Fiber (LPF) with a mode field diameter of 200 μm [17], which is the largest MFA reported to date. However, it is not very versatile because it is a rod-shaped fiber that cannot be adapted to more complex scenarios. Pixelated Bragg fibers were created in 2012 by Assaad Baz [18], [19]. The achieved MFA is 531 μm^2, now considered small for a large

Manuscript received 10 November 2023; accepted 13 November 2023. Date of publication 16 November 2023; date of current version 11 December 2023. This work was supported in part by the National Natural Science Foundation of China under Grant 62075099 and in part by the StateKey Laboratory of Luminescent Materials and Devices, South China University of Technology, Guangzhou under Grant 510640, China (2023-skllmd-16). *(Corresponding authors: Meimei Kong; Wei Wei.)*

The authors are with the College of Electronic and Optical Engineering & College of Flexible electronics (Future Technology), Nanjing University of Posts and Telecommunications, Nanjing 210023, China (e-mail: shenx@njupt.edu.cn; 464189489@qq.com; kongmm@njupt.edu.cn; weiwei@njupt.edu.cn).

Digital Object Identifier 10.1109/JPHOT.2023.3333380

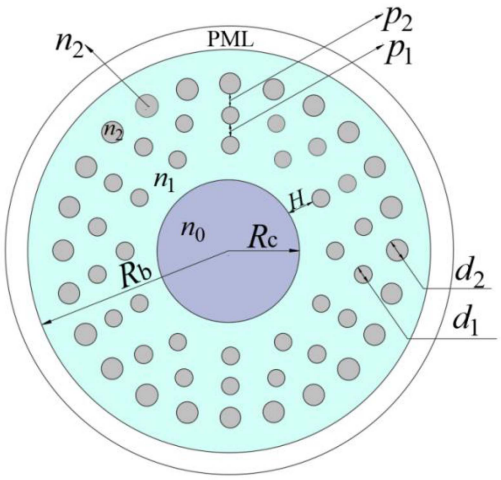

Fig. 1. Schematic diagram of the MLSHRF cross-section.

mode field fiber. A passive leakage channel fiber (LCF) with a 1064 nm wavelength and 1440 μm^2 effective MFA was created by L. Dong et al. in 2007 [20]. In summary, some optical fibers have insufficient MFA, some rely on bending effects to filter out HOMs, and some are not suitable for bending. Therefore, progress remains needed to optimize large-mode-area fibers.

In this study, we present a unique type of large mode area optical fiber for 2.0 μm based on multilayer solid hole resonance, which we denote the MLSHR fiber. We investigate its mode transmission properties in detail, including loss coefficients, mode field area, effective mode field diameter, and power percentage. The MFA is up to 3849 μm^2 in the unbent state with a smaller cladding diameter of 230 μm, and the LR is up to 545. The refractive index and dimension of each circular hole in the cladding can be separately adjusted to suppress HOMs. The fiber structure is solid-state. Compared to reported fibers, our proposed MLSHR fiber proposed has better comprehensive properties and application potential.

II. Fiber Structure and the Theoretical Model

The structure diagram of the MLSHRF is shown in Fig. 1. There are two layers of small solid holes and a layer of large solid holes. The RI of the fiber core is n_0, and the radius is R_c. The distance between the core and the first layer of holes is defined as the core-hole spacing, denoted as H. The layer spacings among the three layers of holes are p_1 and p_2. The RI of the cladding substrate n_1 is 1.4380, and the radius R_b is fixed to 115.0 μm. The RIs of the large and small holes are both n_2, the diameter of the small holes is d_1, and the diameter of the large holes is d_2. The relationship bewteen n_0, n_1 and n_2 is:

$$n_1 < n_0 < n_2 \tag{1}$$

The RI of solid hole n_2 is higher than that of fiber core n_0, the total reflection condition is destroyed, and the signal light transmitted in the fiber core leaks into the surrounding solid holes. Through the mutual adjustment and optimization of the fiber parameters, the loss coefficients of HOMs are much higher than that of FM, so a high loss ratio (LR) is obtained, and HOMs will be filtered out.

Our fiber simulation is based on the full vector finite element method (FEM). The application software is COMSOL Multiphysics. The thickness of the perfectly matched layer (PML) is selected to be five times the wavelength, as shown by the white ring in Fig. 1, and the meshing is extremely fine. Through the calculation of COMSOL software, the effective RI of the fiber is obtained. Thus, the loss coefficient can be calculated by (2) [21]:

$$L = \frac{40\pi}{\ln(10)\lambda}\mathrm{Im}(n_{eff})(dB/m) \tag{2}$$

where $\mathrm{Im}(n_{eff})$ is the imaginary part of the effective RI of the mode and λ is the wavelength. The loss coefficients of the LP_{01} and LP_{11} modes are L_{01} and L_{11}, respectively.

The mode field area (MFA) is an important index to characterize the large mode area fiber, which is expressed as [22]:

$$A_{eff} = \frac{\left(\iint \left|E(x,y)^2\right|\mathrm{d}x\mathrm{d}y\right)^2}{\iint \left|E(x,y)^4\right|\mathrm{d}x\mathrm{d}y} \tag{3}$$

where $E(x, y)$ is the light's transverse electric field component.

The effective mode field diameter (MFD) is expressed as [23]:

$$MFD = \frac{2}{\pi}\sqrt{A_{eff}} = \frac{2\sqrt{2}\int E_i^2(r)\mathrm{d}r}{\left[\int E_i^2(r)\mathrm{d}r\right]^{1/2}} \tag{4}$$

where $E_i(r)$ is the electric field distribution in terms of radial distance r.

Another essential index is called the mode power fraction (PF), which can be beneficial for studying the details of the distribution of optical field energy in the fiber, which is expressed as

$$\eta = \frac{2\int_{core} S_z\mathrm{d}A}{\int_{\mathrm{all}} S_z\mathrm{d}A} \tag{5}$$

where S_z is the Poynting vector extending along the propagation direction, the numerator represents the integral of the fiber core S_z, and the denominator represents the entire fiber S_z. Jorgensen has proved that when the difference between the PF of the LP_{01} and LP_{11} modes is approximately 0.3, the single mode (SM) bandwidth is generated, and the single mode operation can be entirely performed. The SM bandwidth is the region where the first HOM is leaking and couples with cladding modes, while the FM is still confined to the core and has a large fraction of modal power within the core [24], shown in gray shading in the figure below.

III. The Results and Discussion

A. Effects of Small Hole Diameter d_1 on Loss Coefficient

Fig. 2 depicts how d_1 affects the fiber confinement loss and MFA. With an increase in d_1, the loss coefficients rise. Because HOMs leak more than FMs when d_1 grows, more optical power from the core will escape into nearby holes with greater RI. The lowest HOM loss coefficient is better than 10.0 dB/m when d_1 moves from 7.5 to 9.5 μm, and the FM loss coefficient is less than 0.1 dB/m. The outcomes were at a high worldwide level [25]. LR is the ratio of the lowest HOM loss to the FM

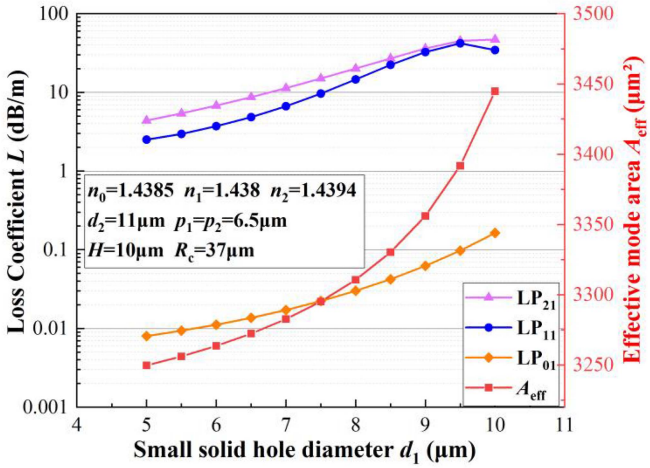

Fig. 2. Effects of d_1 on loss coefficients and MFA.

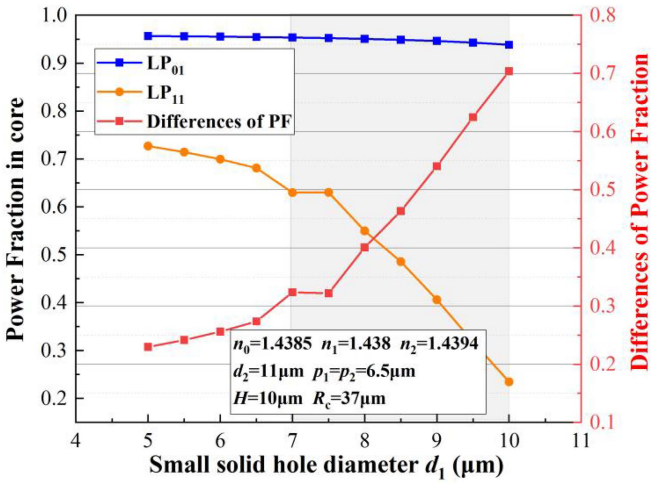

Fig. 3. Effects of d_1 on PF.

loss, and when LR is greater than 100, the fiber is considered a single-mode fiber. For $d_1 = 9.0$ μm, $L_{01} = 0.062$ dB/m, $L_{11} = 32.3$ dB/m, $L_{21} = 36.1$ dB/m, and LR = 517. This suggests that the capacity to discriminate between transverse modes is robust and capable of efficiently filtering out HOMs. MFA rises along with the growth in d_1. The HOMs may better delocalize from the core as a result of the greater d_1 when $A_{eff} = 3356$ μm^2 (MFD = 65.4 μm) and $d_1 = 9.0$ μm, and the lowest HOM loss coefficient is less than 10.0 dB/m when d_1 increases from 5.0 to 7.5 μm. However, single-mode operation may also be attained by lengthening the fiber to filter out HOMs. In this subsection, we can achieve a loss ratio of 517, which allows for better single-mode operation conditions and a larger mode field area than those of the presented article.

The effects of d_1 on PF are shown in Fig. 3. When d_1 changes from 7.0 μm to 10.0 μm, the differences in PF in the core are all larger than 0.3, which is in the SM bandwidth. Therefore, the reasonable range of small hole diameter d_1 is also 7.5–9.5 μm. Compared to past structures using the factor of power fraction, the model proposed in this paper keeps the fundamental mode PF in the core constant under any change in structural parameters.

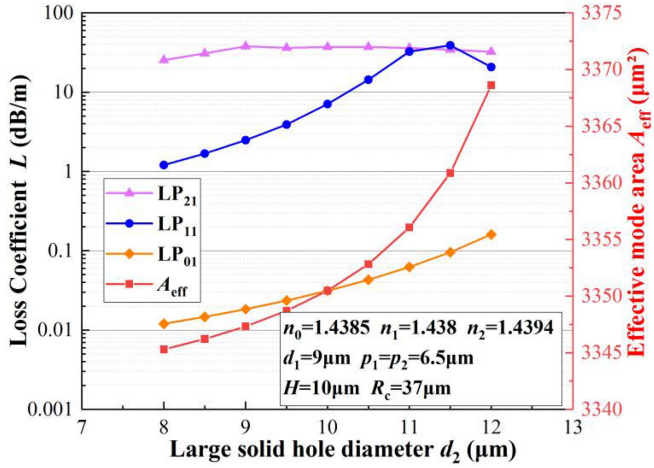

Fig. 4. Effects of d_2 on loss coefficients and MFA.

In other words, the FM in the core does not leak into the cladding and maintains a high PF difference all the time.

B. Effects of Large Hole Diameter d_2 on Loss Coefficient

The effects of the large hole diameter d_2 on the loss coefficients and MFA of the fiber are shown in Fig. 4. The influence trend of d_2 on loss is similar to that of d_1. When d_2 changes from 10.5 μm to 11.5 μm, the lowest HOM loss coefficient is more significant than 10.0 dB/m, and the FM loss coefficient is less than 0.1 dB/m, especially when $d_2 = 11.0$ μm, $L_{01} = 0.062$ dB/m $L_{11} = 32.5$ dB/m, $L_{21} = 36.1$ dB/m, and LR = 521. The transverse mode discrimination ability is very strong when d_2 increases from 8.0 μm to 10.5 μm, and the FM loss coefficient is maintained below 0.1 dB/m. In contrast, the HOM loss coefficient rises from 1.2 dB/m to 14.4 dB/m, so the purpose of single-mode transmission can also be achieved by changing the length of the fiber. When $d_2 = 11.5$ μm and $A_{eff} = 3360$ μm^2 (MFD = 65.8 μm), the MFA increases with increasing d_2.

The effects of the large hole diameter d_2 on PF are shown in Fig. 5. When d_2 increases from 8.0 μm to 11.0 μm, the coupling effect can be better, so the HOM PF decreases in the core. When d_2 increases from 11.0 μm to 12.0 μm, the coupling effect gradually weakens, so the HOM PF increases in the core. The SM bandwidth is 10.0 μm to 11.5 μm, especially when $d_2 = 11.0$ μm, and the PF difference between LP_{01} and LP_{11} reaches a maximum of 0.54, which can most efficiently filter out HOMs and maintain single-mode operation. Thus, d_2 ranges from 10.0 μm to 11.5 μm, and MLSHRF has better mode discrimination ability.

C. Effects of Core Diameter R_c on Loss Coefficient

Fig. 6 shows the effects of the core radius on loss and MFA. These data show that the lowest HOM loss coefficient increases and then decreases when R_c changes from 30.0 μm to 45.0 μm. When R_c changes from 30.0 μm to 40.0 μm, the lowest HOM loss coefficient is greater than 10.0 dB/m, and the FM loss coefficient is less than 0.1 dB/m. When R_c ranges from 30.0 μm to 36.0 μm, the LP_{11} loss gradually increases, the FM loss

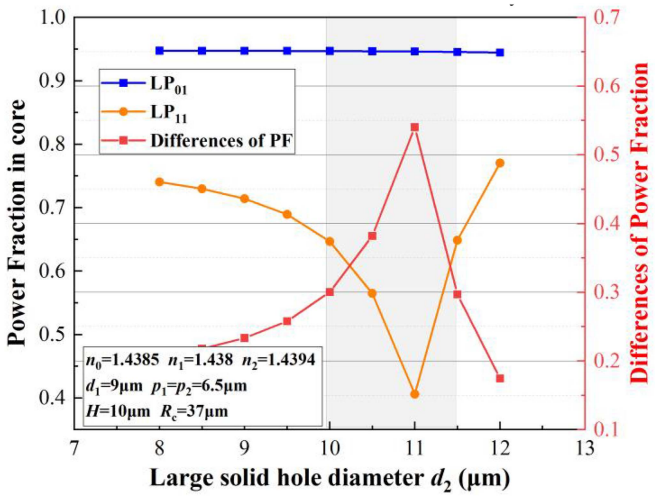

Fig. 5. Effects of d_2 on PF.

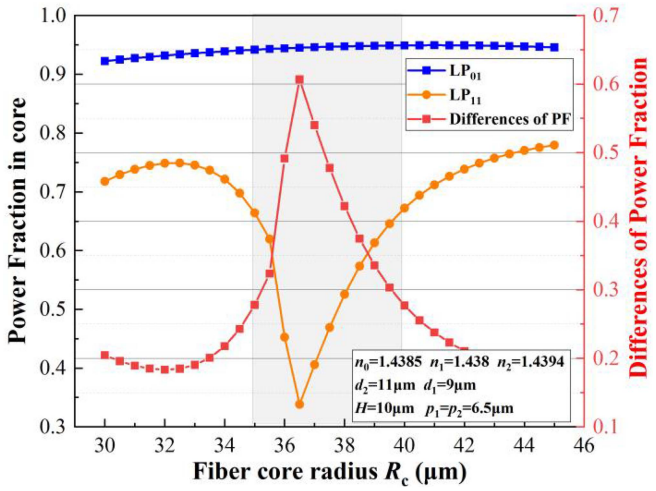

Fig. 7. Effects of R_c on PF.

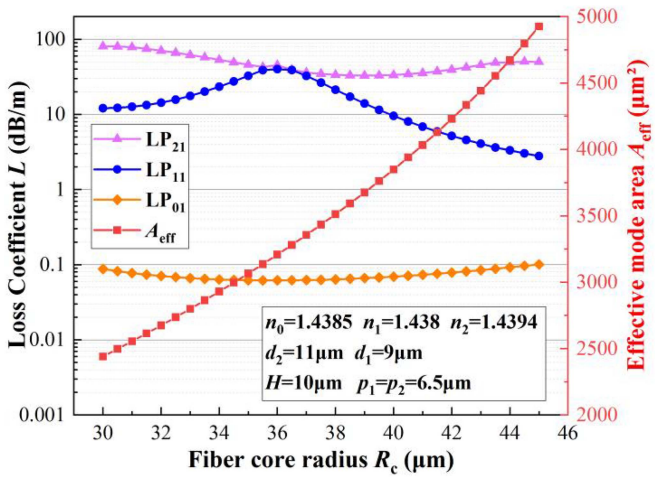

Fig. 6. Effects of R_c on loss coefficients and MFA.

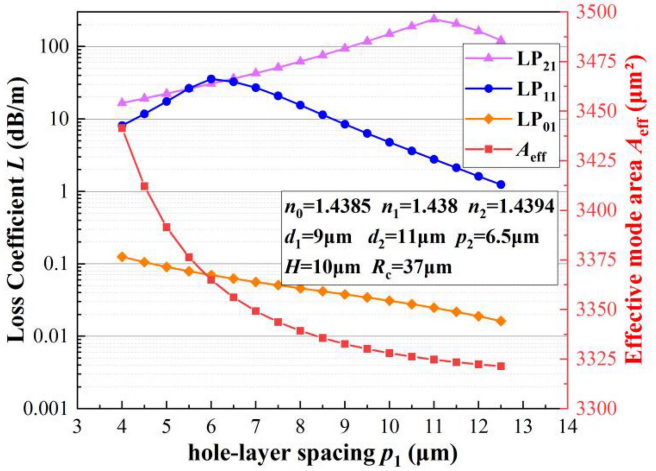

Fig. 8. Effects of p_1 on loss coefficients and MFA.

decreases, L_{11} rises from 12.1 dB/m to 40.1 dB/m, and L_{01} reduces from 0.087 dB/m to 0.062 dB/m. When R_c increases from 36.0 μm to 42.0 μm, the loss of the HOMs decreases from 40.1 dB/m to 5.2 dB/m, but it still has a strong HOM suppression. The maximum LR is at R_c = 36.0 μm. At this point, L_{01} = 0.062 dB/m, L_{11} = 40.1 dB/m, L_{21} = 45.2 dB/m, and LR = 649. When R_c = 40.0 μm, A_{eff} = 3849 μm^2 (MFD = 70.0 μm), which is the largest effective mode field area in this paper. Compared to other fibers in the unbent state, the fiber model can rarely achieve a large mode field area at the same time and maintain a high loss ratio. The advantage of a small fiber diameter is that this design also makes the fiber better adapted to various environmental changes.

The effect of the core radius on the PF is shown in Fig. 7. The SM bandwidth of R_c ranges from 35.0 μm to 40.0 μm. The coupling effect is not obvious for Rc before 36. 5 μm because Rc is small and H is larger. Rc increases gradually after R_c is greater than 36.5 μm, and the HOMs will be confined in the core. Therefore, when R_c ranges from 35.0 μm to 40.0 μm, the MLSHRF has a strong mode discrimination ability and better performs single-mode operation, such that the single-mode core diameter can reach up to 80 μm. At Rc = 36.5 μm, the small hole produces the best coupling effect to the core, driving the HOMs out of the core and into the cladding, with the lowest PF = 0.27 and the highest PF difference = 0.61. A difference of this magnitude is rarely reported in other similar works, indicating that our fiber structure is better suited than previous designs to filter out the higher-order modes.

D. Effects of Hole-Layer Spacing p_1 on Loss Coefficient

The effects of hole-layer spacing p_1 on loss and MFA are shown in Fig. 8. With the increase in p_1, the FM loss shows a decreasing trend, while the minimum HOM loss shows a trend of first increasing and then decreasing. When p_1 increases from 5.0 μm to 8.5 μm, the lowest HOM loss coefficient is greater than 10.0 dB/m, and the FM loss coefficient is less than 0.1 dB/m, especially when p_1 = 6.5 μm, L_{01} = 0.062 dB/m, L_{11} = 32.5 dB/m, L_{21} = 36.1 dB/m, and LR = 521. When p_1 = 5.0 μm, A_{eff} = 3391 μm^2 (MFD = 65.7 μm). When p_1 increases, the MFA decreases gradually. When p_1 increases from 4.0 μm to 6.0 μm, the small hole coupling effect gradually strengthens. L_{11} increases from 8.1 dB/m to 35.5 dB/m, and

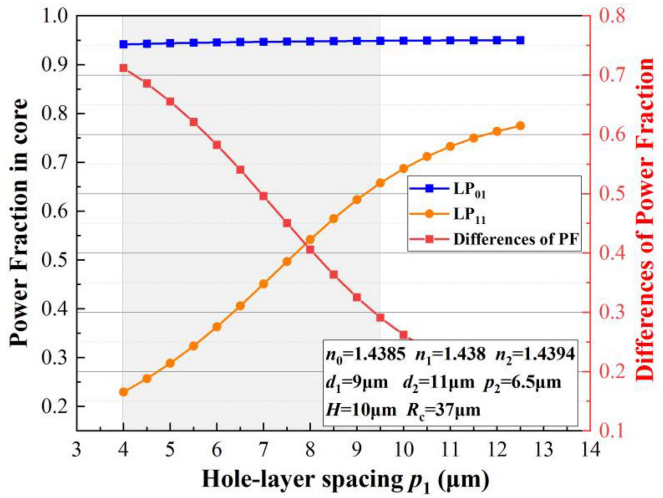

Fig. 9. Effects of p_1 on PF.

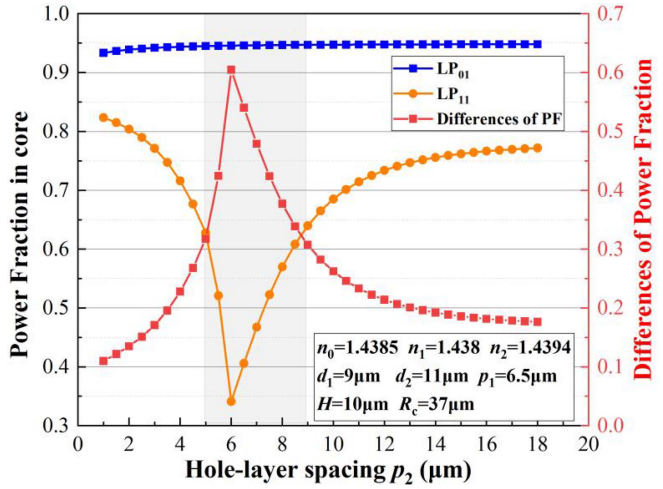

Fig. 11. Effects of p_2 on PF.

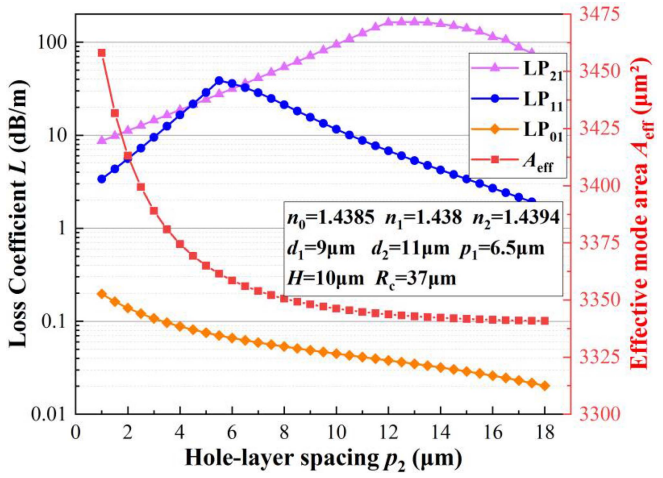

Fig. 10. Effects of p_2 on loss coefficients and MFA.

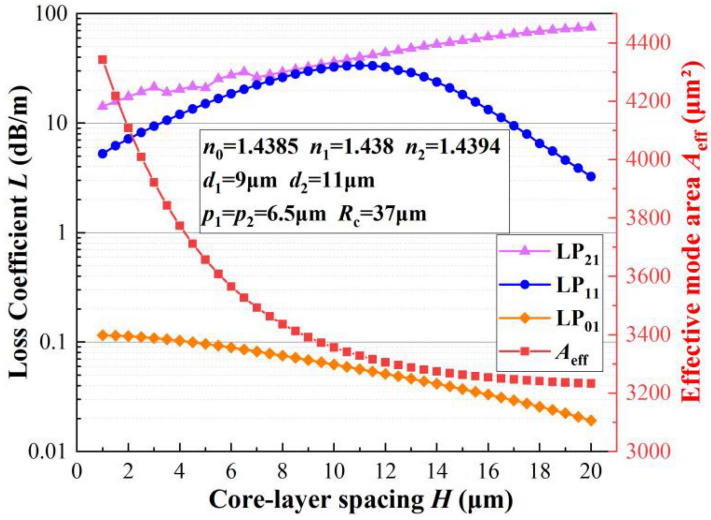

Fig. 12. Effects of H on loss coefficients and MFA.

L_{01} decreases from 0.125 dB/m to 0.061 dB/m. When p_1 is in the range of 6 μm to 12.5 μm, the coupling effect of the small holes gradually weakens. When $p_1 = 9.5$ μm, $L_{11} = 6.3$ dB/m, and $L_{01} = 0.034$ dB/m, the MLSHRF also has a strong mode discrimination ability.

The influence of p_1 on PF is shown in Fig. 9. When p_1 increases from 4.0 μm to 9.5 μm, it is in the SM bandwidth combined with the range of p_1 obtained in Fig. 8. The range of p_1 here is taken as 5.0 μm to 9.5 μm, and MLSHRF can efficiently filter out HOMs and perform single mode operation.

E. Effects of Hole-Layer Spacing p_2 on Loss Coefficient

The effect of p_2 on the loss and MFA is shown in Fig. 10. Similarly, this section changes the position of the third layer of holes when $p_2 = 5.5$ μm and $p_2 = 6.0$ μm, and the loss of the LP_{01} mode reaches the peak. Nevertheless, the loss of the LP_{21} mode is smaller than that of LP_{11}, and the minimum HOM loss is needed to achieve single-mode operation, so the peak value of the minimum HOM loss should be delayed. When $p_2 = 6.5$ μm, $L_{01} = 0.062$ dB/m, $L_{11} = 32.5$ dB/m, $L_{21} = 36.1$ dB/m, and LR = 521. When $p_2 = 4.0$ μm, $A_{\text{eff}} = 3374$ μm^2 (MFD = 65.5 μm). When $p_2 = 13.0$ μm, $L_{11} = 5.3$ dB/m, and $L_{01} = 0.035$ dB/m, the fiber still has strong HOM suppression. Therefore, excellent single-mode operation can be achieved in the range of p_2 from 3.5 to 10.5 μm.

The effect of p_2 on the power fraction is shown in Fig. 11. The range of the SM bandwidth is from 4.5 μm to 10.0 μm. When p_2 is less than 6 μm, the coupling effect is gradually strengthened with increasing p_2. When p_2 is greater than 6.0 μm, the coupling effect of the large hole to the fiber core is steadily weakened, and the HOMs are gradually constrained in the fiber core. Therefore, combined with the result of Fig. 10, we propose that our device can achieve excellent single-mode operation in the 4.0 to 10.0 μm range.

F. Effects of Core-Hole Spacing H on Loss Coefficient

The influence of H on the loss and MFA is shown in Fig. 12. When H is in the range of 3.5 μm to 16.5 μm, MLSHRF can achieve better HOM suppression and perform single-mode

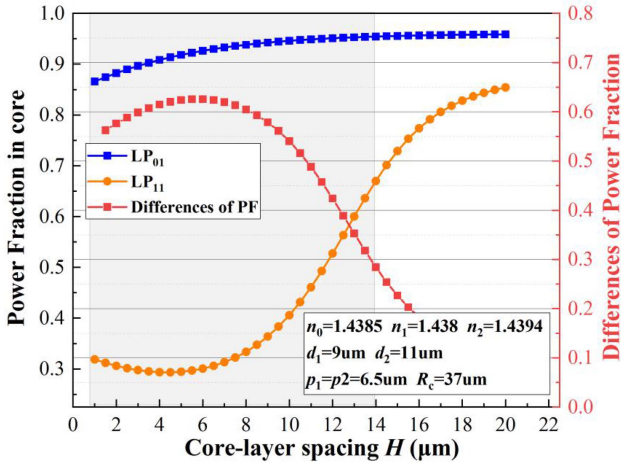

Fig. 13. Effects of H on PF.

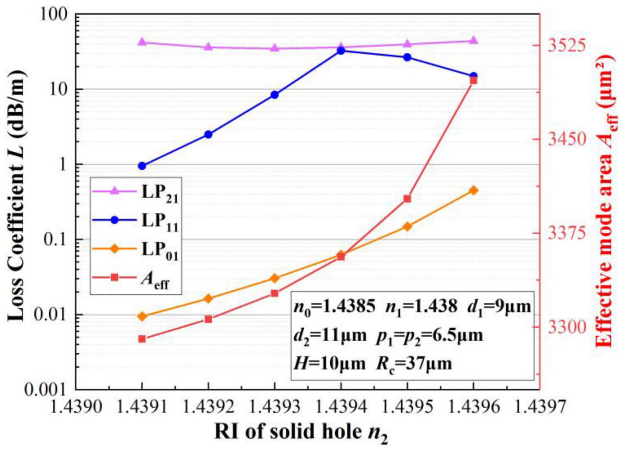

Fig. 14. Effects of n_2 on loss coefficients and MFA.

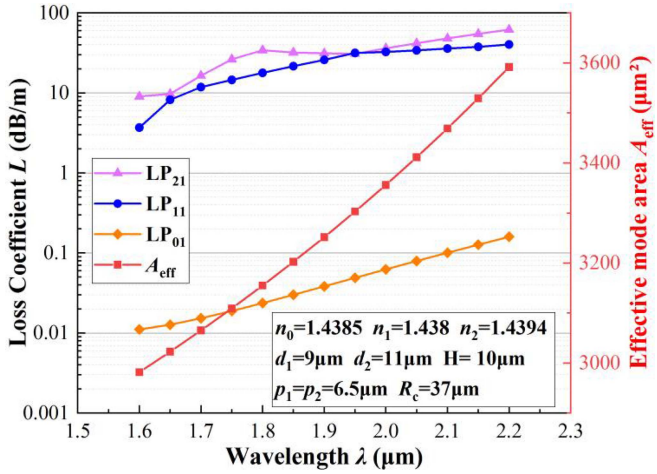

Fig. 15. Effects of λ on loss coefficients and MFA.

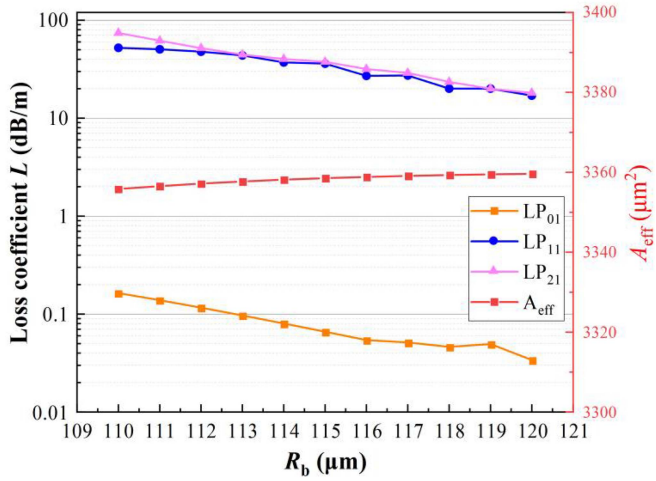

Fig. 16. Effects of R_b on loss coefficients and MFA.

operation, especially when $H = 11.0$ μm, $L_{01} = 0.057$ dB/m, $L_{11} = 33.7$ dB/m, and LR = 595. The MFA decreases with increasing H, and the largest Aeff is 3843 μm^2 (MFD = 69.9 μm) when $H = 3.5$ μm. The variation range of H is extensive, so the fiber has some adaptability to diverse applications.

The effect of H on the PF is shown in Fig. 13. The range of SM bandwidth is from 1.0 μm to 14.0 μm, but considering the result of Fig. 12, we propose that it can achieve even better HOM suppression and perform single-mode operation in a range of 3.5–14.0 μm.

G. Effects of the Refractive Index of Solid Hole n2 on the Loss Coefficient

After optimizing the refractive index of the solid hole, it is found that when $n_2 = 1.4394$, the fiber loss performance is the best, as shown in Fig. 14. Under this condition, $L_{01} = 0.062$ dB/m, $L_{11} = 32.5$ dB/m, $L_{21} = 36.0$ dB/m, and $A_{\text{eff}} = 3356$ μm^2 (MFD = 65.4 μm). When $n_2 = 1.4393$, it can also suppress HOM loss, $L_{01} = 0.03$ dB/m, $L_{11} = 8.4$ dB/m, and $L_{21} = 39.5$ dB/m. Therefore, we propose that the refractive index of n_2 can realize values of 1.4393 and 1.4394.

H. Effects of Wavelength λ on Loss Coefficient

MLSHR is a large mode area fiber designed for 2.00 μm fiber lasers. The effects of the operating wavelength λ on the loss and MFA are shown in Fig. 15. In practice, the wavelength in the experiment will change and have certain errors, so this section simulates the impact of the wavelength change near 2.00 μm on the performance. Fig. 14 shows that when λ is in the range of 1.65 μm to 2.10 μm, L11 increases from 8.2 dB/m to 35.9 dB/m, L01 increases from 0.012 dB/m to 0.104 dB/m, the HOM loss can be stably suppressed, and single-mode operation can be performed in a wide operating wavelength range.

I. Effects of Cladding Radius R_b on Loss Coefficient

The effect of the cladding radius on the fiber performance is shown in Fig. 16. When the radius of the fiber cladding increases, the loss of FM and HOMs all decreases, and the MFA is stable. In fact, the fiber can maintain single mode transmission characteristics when $R_b > 113.0$ μm. In particular, when $R_b = 115.0$ μm, $L_{11} = 36.0$ dB/m, and $L_{01} = 0.066$ dB/m, there is a maximum of LR = 545, and in other cases, the loss ratio is slightly less than this value. A smaller cladding radius helps

TABLE II
EFFECT OF FIBER PARAMETERS ON PERFORMANCE

Parameters	Value (μm)	Transmission characteristics			
		L_{01} (dB/m)	L_{11} (dB/m)	LR	A_{eff} (μm^2)
d_1	7.0	0.017	6.7	392	3283
	9.5	0.097	42.0	433	3392
d_2	10.0	0.031	7.1	228	3353
	11.5	0.095	39.1	411	3361
p_1	5.0	0.090	17.5	189	3391
	9.5	0.034	6.3	185	3330
p_2	4.0	0.088	16.5	182	3374
	10.0	0.045	11.6	245	3346
R_c	35.0	0.062	32.7	516	3065
	40.0	0.069	9.6	139	3849
H	3.5	0.10	10.6	100	3843
	14.0	0.042	23.8	548	3274
λ	1.65	0.012	8.2	684	3022
	2.10	0.10	35.9	360	3469
R_b	113	0.10	43.7	430	3358
	120	0.034	17.0	500	3359

the fiber achieve bending characteristics and is more conducive to manufacturing. Therefore, we propose that $R_b = 115$ μm is the best choice. At the same time, we summarize the simulation parameters carried out above, as shown in Table II, which lists the upper and lower limits of the reasonable range of the parameters. All the parameters have a certain adaptive range, and the area of the mode field fluctuates within a reasonable range. These parameters can also satisfy the high loss ratio when an error occurs and filter out the HOMs easily to realize single-mode operation.

J. Effects of the Refractive Index of Solid Hole n2 on the Loss Coefficient

This section will further illustrate the effect of different air holes in the MLSHRF and their corresponding layer spacings on the fiber performance. We first discuss the small hole d_1 and its corresponding hole-layer spacing p_1. Closer to the fiber core, the size and position of the hole will have a resonant coupling effect on the fiber core, making the high-order mode better delocalized from the active region. Fig. 17(a) and (b) show that with increasing d_1 and p_1, the highest loss of FM and the lowest loss of HOM both increase.

The variation in the FM loss occurs because with increasing d_1, an excessively high refractive index in the small hole will affect the confinement of the fundamental mode. The rise of p_1 can delay this phenomenon, so the FM trend presents a slanted line. In the same way, with increasing d_1, the resonance effect of the small hole on the core is enhanced; these high HOMs are no longer confined to the core, so we can see that a deeper color appears on the right side of the figure. The mode field area also increases with increasing d_1, as shown in Fig. 17(c). The loss ratio reaches its maximum value at $d_1 = 8.0$–8.5 μm and $p_1 = 7.0$–8.0 μm, as shown in Fig. 17(d). In the whole range, the

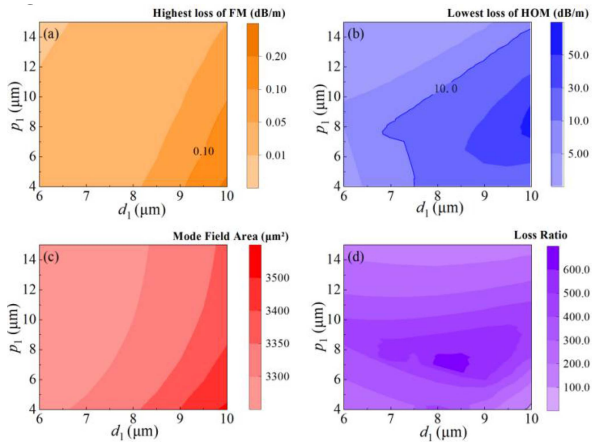

Fig. 17. Deviation of d_1 and p_1 on fiber performance. (a) Highest loss of FM, (b) lowest loss of HOM, (c) MFA, (d) loss ratio. The structural parameters are set as $R_c = 37.0$ μm, $H = 10.0$ μm, $n_0 = 1.4385$, $n_1 = 1.4380$, and $n_2 = 1.4394$.

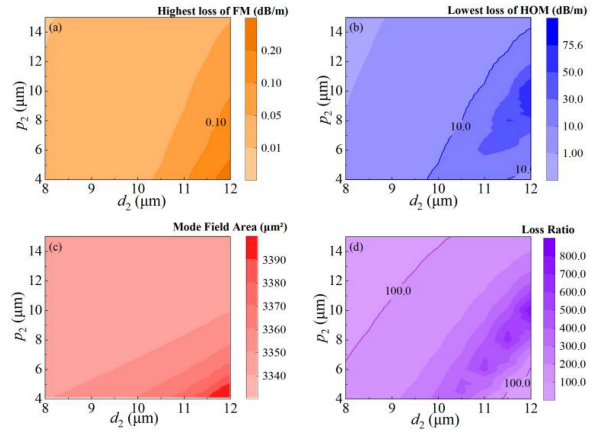

Fig. 18. Deviation of d_2 and p_1 on fiber performance. (a) Highest loss of FM, (b) lowest loss of HOM, (c) MFA, (d) loss ratio. The structural parameters are set as $R_c = 37.0$ μm, $H = 10.0$ μm, $n_0 = 1.4385$, $n_1 = 1.4380$, and $n_2 = 1.4394$.

loss ratio is almost more significant than 100, which can fully realize the good single-mode operation of the fiber.

Second, we discuss the effects of d_2 and p_2 on fiber performance, which can be seen in Fig. 18. Since d_2 is far away from the fiber core, it needs a larger hole diameter to better delocalize HOMs of the fiber core. At the same time, p_2 cannot be too small so that the two layers are gathered together to form a relatively concentrated high refractive index. The ring destroys the resonant coupling effect of the hole on the fiber core. Therefore, p_2 is also appropriately increased. From Fig. 18(a), (b), and (d), we can see that d_2 and p_2 also have a particular impact on the performance of the fiber. When $d_2 = 10.0$–11.5 μm and $p_2 = 8.0$–10.0 μm, it can have a good loss ratio and effective single-mode operation.

IV. OPTICAL FIBER ELECTRIC FIELD DIAGRAM

By calculation, the output mode field distributions of the fiber are shown in Fig. 19. The fiber parameters are $d_1 = 9.0$ μm, $d_2 = 11.0$ μm, $p_1 = 6.5$ μm, $p_2 = 6.0$ μm, $H = 10.0$ μm, and

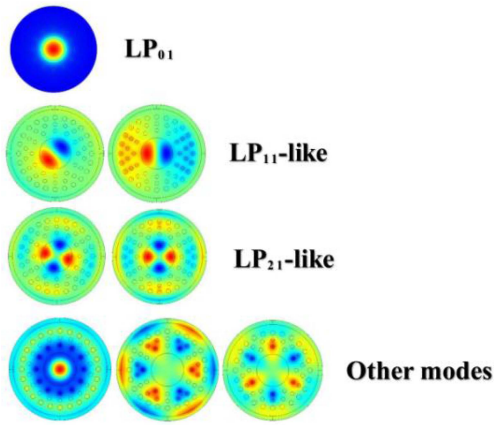

Fig. 19. Mode field distributions of the fiber.

$n_2 = 1.4394$. The LP_{01} mode is entirely confined in the fiber core, the LP_{11} and LP_{21} modes are partially leaked into the solid hole, and other HOMs are dramatically delocalized from the core.

V. Conclusion

In conclusion, this paper presents a novel MLSHRF that can be used at a wavelength of 2.0 μm for single-mode operation. Through two-dimensional finite element simulation technology, the effects of d_1, d_2, p_1, p_2, R_c, H, λ, and n_2 on the transmission performance of the fiber are simulated and analyzed, and the optimized parameter ranges are obtained. The feasible fiber parameter ranges are $d_1 = 7.5$–9.5 μm, $d_2 = 10.0$–11.5 μm, $R_c = 35.0$–40.0 μm, $p_1 = 5.0$–8.5 μm, $p_2 = 4.0$–10.0 μm, $H = 3.5$–14.0 μm and $n_2 = 1.4393$–1.4394. In these ranges, the best parameters of the MLSHRF are $d_1 = 9.0$ μm, $d_2 = 11.0$ μm, $R_c = 37.0$ μm, $p_1 = 6.5$ μm, $p_2 = 6$ μm, $H = 11.0$ μm, and $n_2 = 1.4394$, with $L_{01} = 0.066$ dB/m, $L_{11} = 36.007$ dB/m, and LR $= 545$. The simulation results indicate that the transverse mode discrimination ability of the fiber reaches performance that is comparable to advanced international levels. The tunable working range of the parameters is vast. The diameter of the cladding is rather small compared to competing designs, which facilitates bending. As a result, this device may offer many potential applications in the world of 2.0 μm fiber lasers. The single mode core diameter reaches 80.0 μm, and the corresponding effective mode field area is as high as 3849 μm^2. Because the optical fiber is solid and the cladding diameter is relatively small, it offers the advantages of good heat dissipation, is easy to prepare, bend, cut, and split, and is more conducive to serving applications in high-power fiber lasers.

References

[1] A. Kumar, T. S. Saini, K. D. Naik, and R. K. Sinha, "Large-mode-area single-polarization single-mode photonic crystal fiber: Design and analysis," *J. Appl. Opt.*, vol. 55, no. 19, pp. 4995–5000, 2016.

[2] K. Saitoh et al., "Limitation on effective area of bent large-mode-area leakage channel fibers," *J. Lightw. Technol.*, vol. 29, no. 17, pp. 2609–2615, Sep. 2011.

[3] Y. Zhang et al., "Design and analysis of trench-assisted dual-mode multi-core fiber with large-mode-field-area," *Appl. Opt.*, vol. 60, no. 16, pp. 4698–4705, 2021.

[4] E. Coscelli, C. Molardi, M. Masruri, A. Cucinotta, and S. Selleri, "Thermally resilient Tm-doped large mode area photonic crystal fiber with symmetry-free cladding," *Opt. Exp.*, vol. 22, no. 8, pp. 9707–9714, 2014.

[5] B. Voisiat et al., "Material processing with ultra-short pulse lasers working in 2 μm wavelength range," *Proc. SPIE*, vol. 9350, pp. 120–127, 2015.

[6] D. Jain and J. K. Sahu, "Large mode area single trench fiber for 2 μm operation," *J. Lightw. Technol.*, vol. 34, no. 14, pp. 3412–3417, Jul. 2016.

[7] X. Chen et al., "Leakage channels enabled multi-resonant all-solid photonic bandgap fiber for effective single-mode propagation," *Opt. Exp.*, vol. 29, no. 14, pp. 22455–22469, 2016.

[8] D. Jain, C. Baskiotis, and J. K. Sahu, "Mode area scaling with multi-trench rod-type fibers," *Opt. Exp.*, vol. 21, no. 2, pp. 1448–1455, 2013.

[9] B. M. Kurade, N. Prasad, G. Thavasi Raja, and S. K. Varshney, "Extremely large mode-area compact hybrid multi-trench fiber with controlled leakage loss," in *Proc. IEEE Photon. Conf.*, 2017, pp. 639–640.

[10] S. Ma et al., "Bend-resistant large mode area fiber with an azimuthally segmented trench in the cladding," *J. Lightw. Technol.*, vol. 37, no. 15, pp. 3761–3769, Aug. 2019.

[11] X. Shen, Z. Yang, S. Chen, G. Yang, L. Zhang, and W. Wei, "Fabrication and performance of a heterogeneous-helical-cladding fiber," *IEEE Photon. J.*, vol. 13, no. 4, pp. 1–3, 2021.

[12] X. Chen et al., "Leakage channels enabled multi-resonant all-solid photonic bandgap fiber for effective single-mode propagation," *Opt. Exp.*, vol. 29, no. 14, pp. 22455–22469, 2021.

[13] D. Jain, C. Baskiotis, T. C. May-Smith, J. Kim, and J. K. Sahu, "Large mode area multi-trench fiber with delocalization of higher order modes," *IEEE J. Sel. Topics Quantum Electron.*, vol. 20, no. 5, pp. 242–250, Sep./Oct. 2014.

[14] T. S. Saini, A. Kumar, and R. K. Sinha, "Triangular-core large-mode-area photonic crystal fiber with low bending loss for high power applications," *Appl. Opt.*, vol. 53, no. 31, pp. 7246–7251, 2014.

[15] Z. Guo, L. Pei, T. Ning, J. Zheng, J. Li, and J. Wang, "Resonant-ring assisted large mode area segmented cladding fiber with high-index rings in core," *Opt. Commun.*, vol. 495, 2021, Art. no. 127049.

[16] X. Shen, Z. Yang, X. Xi, Z. Zhang, and W. Wei, "Numerical investigation for the mode transmission characteristics of a large mode area optical fiber with heterogeneous helical claddings designed for 2.0 μm," *Opt. Lett.*, vol. 46, no. 17, pp. 4342–4345, 2021.

[17] A. Steinkopff et al., "Transverse single-mode operation in a passive large pitch fiber with more than 200 μm mode-field diameter," *Opt. Lett.*, vol. 44, no. 3, pp. 650–653, 2019.

[18] A. Baz, G. Bouwmans, L. Bigot, and Y. Quiquempois, "Pixelated high-index ring Bragg fibers," *Opt. Exp.*, vol. 20, no. 17, pp. 18795–18802, 2012.

[19] J. -P. Yehouessi et al., "Low-loss large mode area pixelated and heterostructured Bragg fiber," in *Proc. Eur. Conf. Lasers Electro-Opt.. Opt. Soc. Amer.*, 2015, paper CJ_3_6.

[20] L. Dong, X. Peng, and J. Li, "Leakage channel optical fibers with large effective area," *J. Opt. Soc. Amer. B*, vol. 724, no. 8, pp. 1689–1697, 2007.

[21] J. Wang et al., "Design and analysis for large-mode-area photonic crystal fiber with negative-curvature air ring," *Opt. Fiber Technol.*, vol. 62, 2021, Art. no. 102478.

[22] R. A. Barankov, K. Wei, B. Samson, and S. Ramachandran, "Resonant bend loss in leakage channel fibers," *Opt. Lett.*, vol. 37, no. 15, pp. 3147–3149, 2012.

[23] H. Z. Lv, M. X. Yu, and W. B. Zhong, "Research and design of large-mode area low loss photonic crystal fiber," *Laser Technol.*, vol. 45, no. 2, pp. 196–201, 2021.

[24] X. F. Miao, P. Wu, and B. Y. Zhao, "Optimum design for comb-index core fiber with large mode area," *Infrared Laser Eng.*, vol. 48, no. 9, pp. 197–184, 2019.

[25] K. Miyagi, Y. Namihira, S. M. Abdur Razzak, S. F. Kaijage, and F. Begum, "Measurements of mode field diameter and effective area of photonic crystal fibers by far-field scanning technique," *Opt. Rev.*, vol. 17, no. 4, pp. 388–392, 2010.